Reactionless robust finite-time control for manipulation of passive objects by free-floating space robots

Guo Sheng-Peng(郭胜鹏)†, Li Dong-Xu(李东旭), Meng Yun-He(孟云鹤), and Fan Cai-Zhi(范才智)

College of Aerospace Science and Engineering, National University of Defense Technology, Changsha 410073, *China*

(Received 2 September 2013; revised manuscript received 18 November 2013; published online 25 March 2014)

On-orbit servicing requires efficient techniques for manipulating passive objects. The paper aims at developing a reactionless control method that drives the manipulator to manipulate passive objects with high precision, while inducing no disturbances to its base attitude. To this end, decomposition of the target dynamics from the base dynamics is discussed, so that they can be considered as two independent subsystems. A reactionless nonlinear controller is presented, which ensures high-precision manipulation of the targets and that the base orientation is unchanged. This is achieved by combining the robust finite-time control with the reaction null space. Finally, the performance of the proposed method is examined by comparing it with that of a reactionless PD controller and a pure finite-time controller.

Keywords: reactionless motion, robust finite-time control, on-orbit manipulation

PACS: 45.40.–f, 45.40.Ln, 07.07.Tw **DOI:** 10.1088/1674-1056/23/5/054502

1. Introduction

Robotic on-orbit servicing is of great significance to a growing number of structures that are in orbit.[1] Important tasks such as orbital assembly, construction, etc., require high-precision manipulation of passive objects. On-orbit servicing robots are generally known as free-flying or free-floating space robots.[2] Strong nonlinearity of the system and the complex space environment in orbit complicate the controller design compared to a fixed-based robot on the ground. Moreover, to develop a controller, it is essential to consider the dynamic coupling between the manipulator and the base.[3,4] Therefore, investigating a well-performed control system is a challenging problem for such a system.

Space robots must securely and firmly grasp the passive objects before further manipulation. The capturing operation includes three specific phases: the pre-impact phase, the impact phase, and the post-impact phase.[5] One fundamental constraint during the procedure is keeping the base orientation unchanged. Nenchev and Yoshida[6] originally introduced a reaction null space (RNS) concept to handle the dynamic interaction problem of free-floating robots. Reactionless motion was achieved in the pre- and post-impact phases. More importantly, the RNS-based control approach was verified by engineering test satellite VII flight experiments.[7] Piersigilli *et al.*[8] proposed a reactionless trajectory generation strategy for a two degree-of-freedom space manipulator, which intercepted the target without affecting the base attitude. When interacting with a target initially having angular momentum, the momentum management during the impact phase must be considered. Nenchev and Yoshida[5] studied the impact reactions at the point of momentum transfer and clarified their role for the post-impact motion behavior of the robot. In Refs. [9] and [10], a distributed momentum control strategy was presented, so that all angular momentum was transferred to the reaction wheel after impact. In addition, an optimal control of space manipulators to bring a captured target to rest in the minimum amount of time was developed by Aghili.[11,12] A number of approaches have been presented for the capturing procedure of space robots; however, the actual handling of the firmly grasped passive objects has been studied only a little.[13]

The manipulation of passive objects for on-orbit assembly or construction requires high-precision control of the space robots. Because of the strong nonlinearity of the system, it is hard to obtain an exact dynamics model in practice. A kind of data-driven framework[14,15] is valuable for such a case to achieve more practical oriented results. In view of the complicated space environment, limited manipulating time, and uncertain factors, various studies of the nonlinear control method have been conducted in Refs. [2], [16], and [17]. Most of the reported studies focused on the position and force control of the space manipulators, while a reactionless control method, where the manipulation of passive objects would not disturb its base attitude, has not been studied adequately.

In the paper, a reactionless robust finite-time control method for free-floating space robots is presented. Via the proposed method, the passive objects are manipulated with high precision, meanwhile no disturbances from the manipulation procedure lead to the base attitude. Decomposition of the passive object dynamics from the base attitude dynamics is discussed. Then a robust finite-time controller is developed for the manipulation subtask and the proposed composite controller is derived by combining this controller with the RNS. Finally, simulations are conducted to verify the efficiency of the proposed method. The control performance is compared to

†Corresponding author. E-mail: shengpengg@gmail.com

© 2014 Chinese Physical Society and IOP Publishing Ltd

that of a RNS-PD controller and a pure finite-time controller.

The paper is organized as follows: in Section 2, task space dynamics of the combined system of space robots and targets is derived; in Section 3, the proposed reactionless robust finite-time control method is presented in detail; in Section 4, simulations are conducted to validate the proposed method; finally, conclusions are addressed in Section 5.

2. Dynamics modeling

2.1. Joint space dynamics of free-floating system

Consider an n joints serial-link manipulator mounted on a free-floating spacecraft. Here, it is assumed that the multi-body system is composed of rigid body elements, of which flexible appendages and internal friction effects are neglected. When manipulating, the motion of the manipulator will induce a reaction force to the base body. Such internal force does not impact the spacial position of the mass center of the multi-body system, but changes the position/orientation of the base. However, since the spacecraft always has to point its antennas toward the earth, it is critical to keep the base attitude unchanged. In other words, the base translation is allowed to be disturbed freely but not its attitude.[12] Therefore, in view of constraints to the base attitude, the generalized coordinates of the system under consideration consist of the base angular velocity $\boldsymbol{\omega}_{\rm b} \in \mathcal{R}^3$ and the manipulator joint rates $\dot{\boldsymbol{q}}_{\rm m} \in \mathcal{R}^n$. Without losing generality, the joint space equations governing the motion of the space robots are expressed as follows:[18]

$$\begin{bmatrix} \boldsymbol{H}_{\rm b} & \boldsymbol{H}_{\rm bm} \\ \boldsymbol{H}_{\rm bm}^{\rm T} & \boldsymbol{H}_{\rm m} \end{bmatrix} \begin{bmatrix} \dot{\boldsymbol{\omega}}_{\rm b} \\ \ddot{\boldsymbol{q}}_{\rm m} \end{bmatrix} + \begin{bmatrix} \boldsymbol{c}_{\rm b} \\ \boldsymbol{c}_{\rm m} \end{bmatrix} = \begin{bmatrix} \boldsymbol{\tau}_{\rm b} \\ \boldsymbol{\tau}_{\rm m} \end{bmatrix} + \begin{bmatrix} \boldsymbol{J}_{\rm b}^{\rm T} \\ \boldsymbol{J}_{\rm m}^{\rm T} \end{bmatrix} \boldsymbol{F}_{\rm h}, \quad (1)$$

where $\boldsymbol{H}_{\rm bm} \in \mathcal{R}^{3\times3}$ and $\boldsymbol{H}_{\rm m} \in \mathcal{R}^{n\times n}$ are inertia matrices of the base and the manipulator respectively, $\boldsymbol{H}_{\rm bm} \in \mathcal{R}^{3\times n}$ denotes the coupling inertia matrix between the base and the manipulator, $\boldsymbol{\tau}_{\rm b} \in \mathcal{R}^3$ is the control torque exerted on the centroid of the base, usually generated by the reaction wheels, etc., $\boldsymbol{c}_{\rm b} \in \mathcal{R}^3$ and $\boldsymbol{c}_{\rm m} \in \mathcal{R}^n$ are the nonlinear velocity-dependent terms including the Coriolis and centrifugal force, $\boldsymbol{\tau}_{\rm m} \in \mathcal{R}^n$ is the manipulator joint torque, $\boldsymbol{F}_{\rm h} \in \mathcal{R}^6$ denotes external force and moment exerted on the end-effector, $\boldsymbol{J}_{\rm b} \in \mathcal{R}^{3\times6}$ and $\boldsymbol{J}_{\rm m} \in \mathcal{R}^{n\times6}$ are the Jacobian matrices of the base and the manipulator respectively.

Special interest arises when the system operates in free-floating mode, that is, no active control torque is applied to the base, i.e. $\boldsymbol{\tau}_{\rm b} = 0$. Moreover, it is assumed that no external force or moment is exerted on the system before and after capture. The environmental forces (e.g., micro-gravity, solar pressure) are orders of magnitude much less than the control forces, and hence are not included in the above equation. A respective compensating term would account for these external disturbances in the control law.

Equation (1) describes the dynamics motion of the system when the manipulator is driven in joint space, of which the upper part denotes dynamic coupling between the base attitude and the manipulator. Generally, the spacial position of the end-effector in the task space is the state the variables are concerned with, which are not yet directly included in the dynamic equations. In order to track the end trajectories, equation (1) is transformed from joint space into task space by the following steps.[19]

Let $\dot{\boldsymbol{x}}_{\rm e} = \begin{bmatrix} \boldsymbol{v}_{\rm e} & \boldsymbol{\omega}_{\rm e} \end{bmatrix}^{\rm T} \in \mathcal{R}^6$ be the generalized velocity of the end-effector consisting of the linear and angular velocities, $\boldsymbol{v}_{\rm e}$ and $\boldsymbol{\omega}_{\rm e}$. Then from the system kinematics it is obtained

$$\dot{\boldsymbol{x}}_{\rm e} = \boldsymbol{J}_{\rm b}\boldsymbol{\omega}_{\rm b} + \boldsymbol{J}_{\rm m}\dot{\boldsymbol{q}}_{\rm m}. \quad (2)$$

Upon substitution of $\ddot{\boldsymbol{q}}_{\rm m}$ from the time-derivative of Eq. (2) into Eq. (1), the task space formulation of the free-floating space robots dynamics can be written in the form

$$\begin{bmatrix} \tilde{\boldsymbol{H}}_{\rm b} & \tilde{\boldsymbol{H}}_{\rm be} \\ \tilde{\boldsymbol{H}}_{\rm eb} & \tilde{\boldsymbol{H}}_{\rm e} \end{bmatrix} \begin{bmatrix} \dot{\boldsymbol{\omega}}_{\rm b} \\ \ddot{\boldsymbol{x}}_{\rm e} \end{bmatrix} + \begin{bmatrix} \bar{\boldsymbol{c}}_{\rm b} \\ \bar{\boldsymbol{c}}_{\rm e} \end{bmatrix} = \begin{bmatrix} 0 \\ \boldsymbol{\tau}_{\rm e} \end{bmatrix} + \begin{bmatrix} \boldsymbol{J}_{\rm b}^{\rm T} \\ \boldsymbol{I}_{\rm n} \end{bmatrix} \boldsymbol{F}_{\rm h}, \quad (3)$$

where

$$\begin{cases} \tilde{\boldsymbol{H}}_{\rm b} = \boldsymbol{H}_{\rm b} - \bar{\boldsymbol{H}}_{\rm be}\boldsymbol{J}_{\rm b}, & \bar{\boldsymbol{H}}_{\rm be} = \boldsymbol{H}_{\rm bm}\boldsymbol{J}_{\rm m}^{-1}, & \bar{\boldsymbol{c}}_{\rm b} = \boldsymbol{c}_{\rm b} - \bar{\boldsymbol{H}}_{\rm be}\left(\dot{\boldsymbol{J}}_{\rm b}\boldsymbol{\omega}_{\rm b} + \dot{\boldsymbol{J}}_{\rm m}\dot{\boldsymbol{q}}_{\rm m}\right), \\ \tilde{\boldsymbol{H}}_{\rm eb} = \boldsymbol{J}_{\rm m}^{-\rm T}\boldsymbol{H}_{\rm bm}^{\rm T} - \bar{\boldsymbol{H}}_{\rm e}\boldsymbol{J}_{\rm b}, & \bar{\boldsymbol{H}}_{\rm e} = \boldsymbol{J}_{\rm m}^{-\rm T}\boldsymbol{H}_{\rm m}\boldsymbol{J}_{\rm m}^{-1}, & \bar{\boldsymbol{c}}_{\rm e} = \boldsymbol{J}_{\rm m}^{-\rm T}\boldsymbol{c}_{\rm m} - \bar{\boldsymbol{H}}_{\rm e}\left(\dot{\boldsymbol{J}}_{\rm b}\boldsymbol{\omega}_{\rm b} + \dot{\boldsymbol{J}}_{\rm m}\dot{\boldsymbol{q}}_{\rm m}\right), \end{cases}$$

and vector $\boldsymbol{\tau}_{\rm e} = \boldsymbol{J}_{\rm m}^{-\rm T}\boldsymbol{\tau}_{\rm m}$ denotes the equivalent virtual torque exerted on the end-effector.

2.2. Dynamics of combined system of space robot and target

Equation (3) provides a description of the dynamic behavior of the end-effector and the base in the task space. As we are interested in the dynamics in terms of the generalized velocities of the base and the target, the capturing operation is out of the scope of the paper and will not be discussed here. It is assumed that the target has been locked after capture (as Fig. 1), so that there is no relative motion between the end-effector and the target.

Under the assumption of a rigid-body target, the generalized velocity vector can be defined by $\dot{\boldsymbol{x}}_{\rm t} = \begin{bmatrix} \boldsymbol{v}_{\rm t} & \boldsymbol{\omega}_{\rm t} \end{bmatrix}^{\rm T} \in \mathcal{R}^6$, where $\boldsymbol{v}_{\rm t}$ and $\boldsymbol{\omega}_{\rm t}$ denote linear and angular velocities of the center of mass of the target. Then its dynamics motion in the task space is described by

$$\boldsymbol{F}_{\rm h} = -\boldsymbol{A}_{\rm t}^{-\rm T}\left(\boldsymbol{H}_{\rm t}\ddot{\boldsymbol{x}}_{\rm t} + \boldsymbol{c}_{\rm t}\right), \quad (4)$$

where $\boldsymbol{F}_{\rm h}$ is the internal force vector between the end-target contact point,

$$\boldsymbol{H}_{\rm t} = \begin{bmatrix} m_{\rm t}\boldsymbol{I}_3 & 0 \\ 0 & \boldsymbol{I}\boldsymbol{I}_{\rm t} \end{bmatrix}$$

is the target inertia matrix with $m_{\rm t}$ and $\boldsymbol{I}\boldsymbol{I}_{\rm t}$ being the mass and inertia tensor respectively,

$$\boldsymbol{c}_{\rm t} = \begin{bmatrix} m_{\rm t}\boldsymbol{\omega}_{\rm t} \times \boldsymbol{v}_{\rm t} \\ \boldsymbol{\omega}_{\rm t} \times \boldsymbol{I}\boldsymbol{I}_{\rm t}\boldsymbol{\omega}_{\rm t} \end{bmatrix}$$

is the nonlinear term, and

$$\boldsymbol{A}_{\rm t} = \begin{bmatrix} \boldsymbol{I}_3 & \boldsymbol{\rho}^{\times} \\ 0 & \boldsymbol{I}_3 \end{bmatrix}$$

is a transformation matrix from the contact point to the centroid of the target with $\boldsymbol{\rho}$ being the position vector of the contact point.

Furthermore, the generalized velocities $\dot{\boldsymbol{x}}_{\rm e}$ and $\dot{\boldsymbol{x}}_{\rm t}$ are related by the following:

$$\dot{\boldsymbol{x}}_{\rm t} = \boldsymbol{A}_{\rm t}\dot{\boldsymbol{x}}_{\rm e}. \tag{5}$$

For the combined system of space robots and target, the internal force, $\boldsymbol{F}_{\rm h}$, can be eliminated from Eqs. (3) and (4) to yield the governing equations of the dynamics motion

$$\begin{bmatrix} \tilde{\boldsymbol{H}}_{\rm b} & \tilde{\boldsymbol{H}}_{\rm bt} \\ \tilde{\boldsymbol{H}}_{\rm eb} & \tilde{\boldsymbol{H}}_{\rm t} \end{bmatrix} \begin{bmatrix} \dot{\boldsymbol{\omega}}_{\rm b} \\ \ddot{\boldsymbol{x}}_{\rm t} \end{bmatrix} + \begin{bmatrix} \tilde{\boldsymbol{c}}_{\rm b} \\ \tilde{\boldsymbol{c}}_{\rm t} \end{bmatrix} = \begin{bmatrix} 0 \\ \boldsymbol{\tau}_{\rm e} \end{bmatrix}, \tag{6}$$

with

$$\begin{cases} \tilde{\boldsymbol{H}}_{\rm bt} = \bar{\boldsymbol{H}}_{\rm be}\boldsymbol{A}_{\rm t}^{-1} + \boldsymbol{J}_{\rm b}^{\rm T}\boldsymbol{A}_{\rm t}^{-{\rm T}}\boldsymbol{H}_{\rm t}, & \tilde{\boldsymbol{c}}_{\rm b} = \bar{\boldsymbol{c}}_{\rm b} + \boldsymbol{J}_{\rm b}^{\rm T}\boldsymbol{A}_{\rm t}^{-{\rm T}}\boldsymbol{c}_{\rm t}, \\ \tilde{\boldsymbol{H}}_{\rm t} = \bar{\boldsymbol{H}}_{\rm e}\boldsymbol{A}_{\rm t}^{-1} + \boldsymbol{A}_{\rm t}^{-{\rm T}}\boldsymbol{H}_{\rm t}, & \tilde{\boldsymbol{c}}_{\rm t} = \bar{\boldsymbol{c}}_{\rm e} + \boldsymbol{A}_{\rm t}^{-{\rm T}}\boldsymbol{c}_{\rm t}. \end{cases}$$

The aforementioned assumption that no external forces, except the internal driving torques to the manipulator joints, act on the system holds in Eq. (6). It is shown that control commands in joint space result in a dynamic response of the target and the base. However, disturbances to the base attitude are not permitted in practice. On the other hand, the dynamic coupling can be applied to adjust the base attitude.[20,21] Furthermore, it is possible to simultaneously control the motion of the target and the attitude of the base if the manipulator has kinematic redundancy with respect to the task.[6,22] Therefore, the objective is to develop a coordination controller in order to manipulate the target without changing the base attitude.

2.3. The reaction null space

The upper part of Eq. (6) can be reformulated as

$$\tilde{\boldsymbol{H}}_{\rm b}\dot{\boldsymbol{\omega}}_{\rm b} + \tilde{\boldsymbol{c}}_{\rm bb}\boldsymbol{\omega}_{\rm b} = -\tilde{\boldsymbol{H}}_{\rm bt}\ddot{\boldsymbol{x}}_{\rm t} - \tilde{\boldsymbol{c}}_{\rm bt}\dot{\boldsymbol{x}}_{\rm t}. \tag{7}$$

The right-hand side of Eq. (7) represents the reaction force and moment applied to the base by the motion of the target. Consequently, if the appropriate acceleration for zero reaction force is computed, the base attitude will not be disturbed. Without losing generality, we assume that the system is initially at rest. Solving Eq. (7) for the reactionless acceleration obtains

$$\ddot{\boldsymbol{x}}_{\rm t} = -\tilde{\boldsymbol{H}}_{\rm bt}^{+}\tilde{\boldsymbol{c}}_{\rm b} + \left(\boldsymbol{I}_3 - \tilde{\boldsymbol{H}}_{\rm bt}^{+}\tilde{\boldsymbol{H}}_{\rm bt}\right)\ddot{\boldsymbol{x}}_{\xi}, \tag{8}$$

where $(\cdot)^{+}$ denotes the right pseudo-inverse of the inertia coupling matrix, $\ddot{\boldsymbol{x}}_{\xi} \in \mathcal{R}^6$ is an arbitrary acceleration vector, $\boldsymbol{P}_{\rm RNS} = \left(\boldsymbol{I}_3 - \tilde{\boldsymbol{H}}_{\rm bt}^{+}\tilde{\boldsymbol{H}}_{\rm bt}\right)$ stands for the projector onto the null space of the inertia coupling matrix $\tilde{\boldsymbol{H}}_{\rm bt}$. Since $\tilde{\boldsymbol{H}}_{\rm bt}\boldsymbol{P}_{\rm RNS}$ is strictly zero, it is easy to verify that dynamics motion (Eq. (8)) results in zero reaction to the base attitude, so that the null space of $\tilde{\boldsymbol{H}}_{\rm bt}$ is named as the reaction null space (RNS).[7] As mentioned above, the existence condition for RNS is kinematic redundancy of the manipulator.[10,23] Full decoupling of the target dynamics from the base dynamics is achieved in the presence of the RNS. Therefore, the concept can be applied to develop a reactionless controller.

3. Reactionless robust finite-time control

The objective of the work is to develop a coordination controller that sends commands to the manipulator in order to fulfill passive objects manipulation, but not to disturb the base attitude. To this end, it is assumed the manipulator is kinematically redundant. Hence referring to the RNS, control torques at the joint level can be divided into two dynamically decoupled vectors: torques that control the dynamics motion of the target, and torques that compensate for the disturbance to base attitude. In practice, these two control tasks could be performed simultaneously.[10,24]

3.1. Compensation for base motion

The reactionless target acceleration in task space is designed via the upper part of Eqs. (6) and (8) as

$$\ddot{\boldsymbol{x}}_{\rm t}^{\rm d} = -\tilde{\boldsymbol{H}}_{\rm bt}^{+}\tilde{\boldsymbol{H}}_{\rm b}\dot{\boldsymbol{\omega}}_{\rm b} - \tilde{\boldsymbol{H}}_{\rm bt}^{+}\tilde{\boldsymbol{c}}_{\rm b} + \boldsymbol{P}_{\rm RNS}\ddot{\boldsymbol{x}}_{\xi}. \tag{9}$$

The manipulator is finally driven by joint torques to achieve the desired tasks. The decoupled control laws corresponding to the base motion task and the target motion task are represented by $\boldsymbol{u}_{\rm b}$ and $\boldsymbol{u}_{\rm t}$ respectively. Then the joint control torques can be computed by substituting the control acceleration (Eq. (9)) into the lower part of Eq. (6)

$$\begin{aligned} \boldsymbol{\tau}_{\rm m} = {} & \boldsymbol{J}_{\rm m}^{\rm T}\left(\tilde{\boldsymbol{H}}_{\rm eb} - \tilde{\boldsymbol{H}}_{\rm t}\tilde{\boldsymbol{H}}_{\rm bt}^{+}\tilde{\boldsymbol{H}}_{\rm b}\right)\boldsymbol{u}_{\rm b} + \boldsymbol{J}_{\rm m}^{\rm T}\tilde{\boldsymbol{H}}_{\rm t}\boldsymbol{P}_{\rm RNS}\boldsymbol{u}_{\rm t} \\ & + \boldsymbol{J}_{\rm m}^{\rm T}\left(\tilde{\boldsymbol{c}}_{\rm t} - \tilde{\boldsymbol{H}}_{\rm t}\tilde{\boldsymbol{H}}_{\rm bt}^{+}\tilde{\boldsymbol{c}}_{\rm b}\right). \end{aligned} \tag{10}$$

The first term on the right-hand side of Eq. (10) guarantees to eliminate the angular momentum from the base. The second term accounts for the desired manipulation of the target, and the last one is a compensation for the system nonlinear parts.

One of the primary tasks is to keep the base orientation unchanged. In order to achieve that, a control law $\boldsymbol{u}_{\rm b}$ is designed as

$$\boldsymbol{u}_{\rm b} = -\boldsymbol{K}_{\rm d}\boldsymbol{\omega}_{\rm b}, \tag{11}$$

where $\boldsymbol{K}_{\mathrm{d}}$ is a gain matrix for base motion damping.

Control torques from Eqs. (10) and (11) guarantee approximately zero base rotation, given properly chosen gains. Next, $\boldsymbol{u}_{\mathrm{t}}$ is designed not only to track desired trajectories precisely in task space, but also to account for the aforementioned external disturbances, such that a robust control method is developed.

3.2. Nonlinear control of the target

Definition 1 For any vector $\boldsymbol{y} \in \mathcal{R}^n$ and $\sigma = \sigma_1/\sigma_2$, $\sigma_2 > \sigma_1 > 0$ are odd integers

$$\mathrm{sig}_{\sigma}(\boldsymbol{y}) = \left[\, \mathrm{sgn}(y_1)\cdot|y_1|^{\sigma} \quad \mathrm{sgn}(y_2)\cdot|y_2|^{\sigma} \quad \cdots \quad \mathrm{sgn}(y_n)\cdot|y_n|^{\sigma} \,\right]^{\mathrm{T}},$$

where $\mathrm{sgn}(\cdot)$ represents sign function.

Let $\boldsymbol{x}_{\mathrm{d}} = \left[\, \boldsymbol{r}_{\mathrm{b}}^{\mathrm{d}} \;\; \boldsymbol{\theta}_{\mathrm{b}}^{\mathrm{d}} \,\right]^{\mathrm{T}} \in \mathcal{R}^6$ be the desired spatial position in task space, and $\dot{\boldsymbol{x}}_{\mathrm{d}}$, $\ddot{\boldsymbol{x}}_{\mathrm{d}}$ be the corresponding velocity and acceleration. Here we define a reference velocity as

$$\dot{\boldsymbol{x}}_{\mathrm{r}} = \dot{\boldsymbol{x}}_{\mathrm{d}} - \boldsymbol{K}_{\alpha}\mathrm{sig}_{\sigma}(\tilde{\boldsymbol{x}}), \tag{12}$$

where $\boldsymbol{K}_{\alpha} \in \mathcal{R}^{6\times 6}$ is a constant diagonal positive-definite matrix, $\tilde{\boldsymbol{x}} = \boldsymbol{x}_{\mathrm{t}} - \boldsymbol{x}_{\mathrm{d}} \in \mathcal{R}^6$ represents the system control error.

The reference acceleration is obtained from the time-derivative of Eq. (12)

$$\ddot{\boldsymbol{x}}_{\mathrm{r}} = \ddot{\boldsymbol{x}}_{\mathrm{d}} - \boldsymbol{K}_{\alpha}\,\mathrm{diag}\left[\sigma\mathrm{sig}_{\sigma-1}(\tilde{\boldsymbol{x}})\right]\dot{\tilde{\boldsymbol{x}}}.$$

The reference error between $\dot{\boldsymbol{x}}_{\mathrm{r}}$ and actual velocity $\dot{\boldsymbol{x}}_{\mathrm{t}}$ can be described by

$$\gamma = \dot{\boldsymbol{x}}_{\mathrm{t}} - \dot{\boldsymbol{x}}_{\mathrm{r}}.$$

Then the trajectory tracking control of the target is determined as

$$\boldsymbol{u}_{\mathrm{t}} = \ddot{\boldsymbol{x}}_{\mathrm{r}} - \left[\boldsymbol{K}_{\phi}\gamma + \boldsymbol{K}_{\beta}\mathrm{sig}_{\sigma_0}(\gamma)\right], \tag{13}$$

where $\boldsymbol{K}_{\phi}$, $\boldsymbol{K}_{\beta} \in \mathcal{R}^{6\times 6}$ are constant diagonal positive-definite matrices, σ_0 is a positive integer which satisfies definition 1.

Finally, substituting Eqs. (11) and (13) into Eq. (10) results in the joint control torques

$$\begin{aligned}\boldsymbol{\tau}_{\mathrm{m}} \;=\; & -\boldsymbol{J}_{\mathrm{m}}^{\mathrm{T}}\left(\tilde{\boldsymbol{H}}_{\mathrm{eb}} - \tilde{\boldsymbol{H}}_{\mathrm{t}}\tilde{\boldsymbol{H}}_{\mathrm{bt}}^{+}\tilde{\boldsymbol{H}}_{\mathrm{b}}\right)\boldsymbol{K}_{\mathrm{d}}\boldsymbol{\omega}_{\mathrm{b}} \\ & + \boldsymbol{J}_{\mathrm{m}}^{\mathrm{T}}\tilde{\boldsymbol{H}}_{\mathrm{t}}\boldsymbol{P}_{\mathrm{RNS}}\left[\ddot{\boldsymbol{x}}_{\mathrm{r}} - \boldsymbol{K}_{\phi}\gamma - \boldsymbol{K}_{\beta}\mathrm{sig}_{\sigma_0}(\gamma)\right] \\ & + \boldsymbol{J}_{\mathrm{m}}^{\mathrm{T}}\left(\tilde{\boldsymbol{c}}_{\mathrm{t}} - \tilde{\boldsymbol{H}}_{\mathrm{t}}\tilde{\boldsymbol{H}}_{\mathrm{bt}}^{+}\tilde{\boldsymbol{c}}_{\mathrm{b}}\right).\end{aligned} \tag{14}$$

3.3. Stability analysis

Proposition Consider a free-floating space robot dynamics governed by Eq. (6), if the manipulator joint control law is designed as Eq. (14), the task space trajectory tracking errors will converge to zero in finite time, meanwhile, the base attitude will remain at the initial orientation.

Proof Substituting the above control law into system dynamics as Eq. (6), target acceleration $\ddot{\boldsymbol{x}}_{\mathrm{t}}$ is eliminated so as to obtain the closed-loop attitude equation

$$\begin{aligned}&\left(\tilde{\boldsymbol{H}}_{\mathrm{b}} - \tilde{\boldsymbol{H}}_{\mathrm{bt}}\tilde{\boldsymbol{H}}_{\mathrm{t}}^{-1}\tilde{\boldsymbol{H}}_{\mathrm{eb}}\right)\left(\dot{\boldsymbol{\omega}}_{\mathrm{b}} + \boldsymbol{K}_{\mathrm{d}}\boldsymbol{\omega}_{\mathrm{b}}\right) \\ &+ \tilde{\boldsymbol{H}}_{\mathrm{bt}}\boldsymbol{P}_{\mathrm{RNS}}\left[\ddot{\boldsymbol{x}}_{\mathrm{r}} - \boldsymbol{K}_{\phi}\gamma - \boldsymbol{K}_{\beta}\mathrm{sig}_{\sigma_0}(\gamma)\right] = 0.\end{aligned} \tag{15}$$

Obviously, the second term of Eq. (15) equals to zero from the RNS. The matrix expression $\left(\tilde{\boldsymbol{H}}_{\mathrm{b}} - \tilde{\boldsymbol{H}}_{\mathrm{bt}}\tilde{\boldsymbol{H}}_{\mathrm{t}}^{-1}\tilde{\boldsymbol{H}}_{\mathrm{eb}}\right)$ is full rank,[6] such that the base rotation will be zero with proper choice of the gain matrix $\boldsymbol{K}_{\mathrm{d}}$.

Since $\tilde{\boldsymbol{H}}_{\mathrm{t}}\boldsymbol{P}_{\mathrm{RNS}}$ is full rank, substituting the possible target acceleration (8) and the control torques (14) into the lower part of Eq. (6) under the condition of a stationary base, obtains the closed-loop equation of the target

$$\ddot{\boldsymbol{x}}_{\mathrm{t}} - \ddot{\boldsymbol{x}}_{\mathrm{r}} + \boldsymbol{K}_{\phi}\gamma + \boldsymbol{K}_{\beta}\mathrm{sig}_{\sigma_0}(\gamma) = 0. \tag{16}$$

Equation (16) is a nonlinear ordinary differential equation with respect to the parameter γ. The general solution shows that γ goes to the equilibrium point $\gamma = 0$ from arbitrary initial conditions at a certain time t_{γ}[25]

$$t_{\gamma} = \frac{1}{1-\sigma_0}\boldsymbol{K}_{\phi}^{-1}\ln\left[\boldsymbol{K}_{\beta}^{-1}\boldsymbol{K}_{\phi}\gamma(0)^{1-\sigma_0} + 1\right]. \tag{17}$$

Referring to the terminal sliding mode control theory,[26–28] $\gamma = 0$ is a nonlinear sliding mode of the control errors. If properly chosen of the matrices $\boldsymbol{K}_{\phi}$, $\boldsymbol{K}_{\beta}$, system control errors converge rapidly to zero along the sliding mode surface.[29] The external environmental disturbances (eg., gravity gradient, solar pressure), parametric uncertainties, as well as un-modeled dynamics are supposed to be expressed as a bounded time varying function symbolized by $\boldsymbol{d}(t)$, with $\|\boldsymbol{d}(t)\| \le \Gamma$. Thus in order to ensure the robust stability, $\boldsymbol{K}_{\beta}$ holds for

$$\boldsymbol{K}_{\beta} = \frac{\Gamma}{\|\gamma^{\sigma_0}\|} + \delta, \delta > 0.$$

In view of Eq. (12), it is obtained from the sliding surface

$$\dot{\tilde{\boldsymbol{x}}} + \boldsymbol{K}_{\alpha}\mathrm{sig}_{\sigma}(\tilde{\boldsymbol{x}}) = 0. \tag{18}$$

Equation (18) is a first-order nonlinear ordinary differential equation with respect to system control errors. Given that $\boldsymbol{K}_{\alpha}$ and σ satisfy the previous conditions, it is obvious that system control errors $\tilde{\boldsymbol{x}}$ will converge to the stable equilibrium point $\tilde{x} = 0$ at a certain time t_x

$$t_x = \frac{\boldsymbol{K}_{\alpha}^{-1}}{1-\sigma}\left|\tilde{x}(0)\right|^{1-\sigma}. \tag{19}$$

4. Simulations and discussion

4.1. Simulation results

In this section, simulations are conducted by Matlab/Simulink to evaluate the effectiveness of the proposed reactionless robust finite-time control method. Here, we consider a three degrees-of-freedom planar manipulator mounted on a free-floating spacecraft, shown as Fig. 1. Its control mission is to manipulate a passive object from the initial position in Cartesian space to a desired position, while the attitude of the spacecraft cannot be disturbed by the manipulation. The parameters of the space robot system and the target are shown in Table 1.

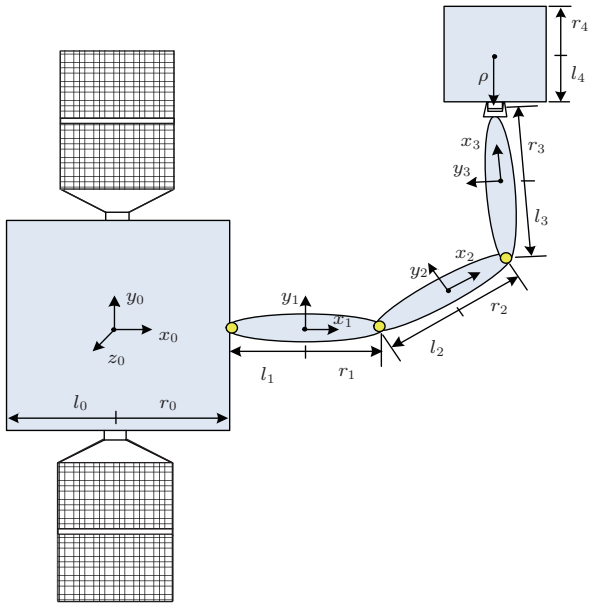


Fig. 1. (color online) A diagram of the space robots and the target.

Table 1. The parameters of the combined system of space robots and target.

	r_i/m	l_i/m	m_i/kg	I_{zi}/(kg·m^2)
Base	1.15	1.15	5799.287	4124.834
Link 1	1	1	68.685	22.844
Link 2	1	1	68.685	22.844
Link 3	0.85	0.85	54.948	19.417
Target	0.3	0.3	50.301	3.018

As discussed before, only the translational position of the target is controlled in order to make sure the manipulator is redundant with respect to the task. A stationary initial state of the combined system is assumed. The inertial frame coincides with the mass center of the entire system.

The initial attitude of the system: $\left[\, Q_{\rm b} \;\; \boldsymbol{q}_{\rm m} \,\right]^{\rm T} = \left[\, 0 \;\; -10^0 \;\; 20^0 \;\; 10^0 \,\right]^{\rm T}$. The desired position of the target: $\boldsymbol{x}_{\rm d} = \left[\, 3 \;\; -2 \,\right]^{\rm T}$. The system uncertainties and the external disturbances are expressed by

$$\boldsymbol{d}(t) = 0.1\left[\sin\left(\dot{\boldsymbol{q}}_{\rm m} t\right) + \cos\left(\dot{\boldsymbol{q}}_{\rm m} t\right)\right].$$

The proposed reactionless robust finite-time control (RRFTC) method is applied to such a system. The parameters of the controller are as follows:

$$\sigma = 3/5, \quad \sigma_0 = 1/3, \quad \boldsymbol{K}_\alpha = \mathrm{diag}\left[\, 1 \;\; 1 \,\right],$$
$$\boldsymbol{K}_\phi = \mathrm{diag}\left[\, 10 \;\; 10 \,\right],$$
$$\boldsymbol{K}_{\rm d} = \mathrm{diag}\left[\, 10 \;\; 10 \,\right], \quad \delta = 1.$$

For the purpose of comparison, the robust finite-time control (RFTC) without considering constraint to the base attitude and the reactionless PD (RPD) control are applied to the same system. The corresponding parameters of them are the same as the above. Finally, the simulation results are shown in Figs. 2–11.

4.2. Discussion

Figure 2 shows the actual trajectories of the target manipulated by the space robots, where the solid line is the simulation result of the RRFTC, and the dotted line is that of the RPD. In addition, the snapshots animation from the result of RRFTC is shown in Fig. 2. It can be seen that in all cases the target is manipulated to the desired position. However, the proposed RRFTC has a much smoother trajectory than the RPD. We can see further from Fig. 3 that the proposed method performs higher precision and convergence rate. As mentioned for RRFTC controller, the time that control errors converge to zero can be calculated from Eqs. (17) and (19).

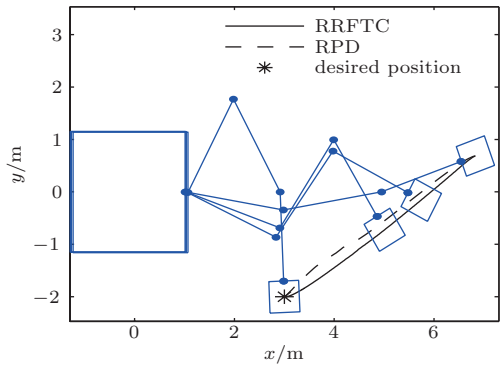


Fig. 2. (color online) The actual trajectories of target and the snapshot animations from the result of RRFTC.

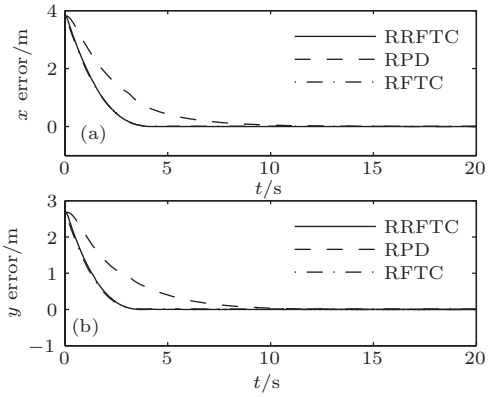


Fig. 3. The trajectory tracking errors: (a) x error. (b) y error.

From Figs. 2 and 4, it is shown that the base orientation is not disturbed during the manipulation in the cases of RRFTC and RPD. The absolute stability of the base attitude is in the scale of 10^{-6} rad (Fig. 4). However, it is clear that the proposed RRFTC has a shorter settling time, which leads to smaller disturbance to the base attitude in practice.

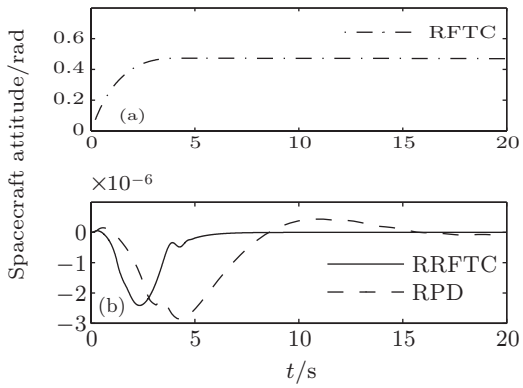


Fig. 4. The trajectories of the base attitude. (a) RFTC. (b) RRFTC and RPD.

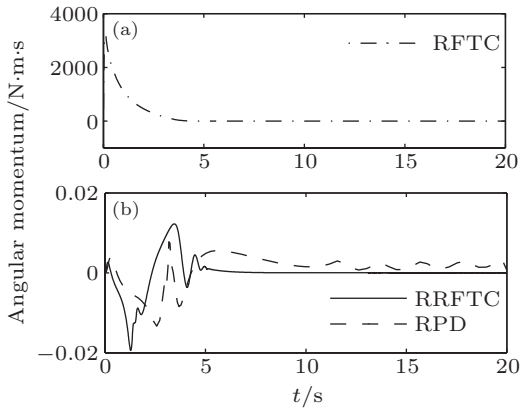


Fig. 5. The trajectories of the angular momentum of the base. (a) RFTC and (b) RRFTC and RPD.

In the case of RFTC, which does not constrain base rotation, the base attitude deviates from its initial position by 0.47 rad (Fig. 4), though the control performance is as good as the case of RRFTC (Fig. 3). Figure 5 shows the angular momentum of the base with respect to time. It is seen clearly that the whole manipulation process in RRFTC is reactionless and more stable.

The joint space trajectories of the manipulator are shown in Figs. 6–8 respectively. It is seen from Figs. 6 and 7 that the final configurations of the manipulator are almost the same, but the trajectories in Fig. 6 are more stable. In other words, the proposed method provides a smother path for manipulation. The trajectories in Figs. 6 and 8 correspond to the same path in the task space (Fig. 3). However, motions in joint space are recalculated when the base attitude constraints are taken into consideration.

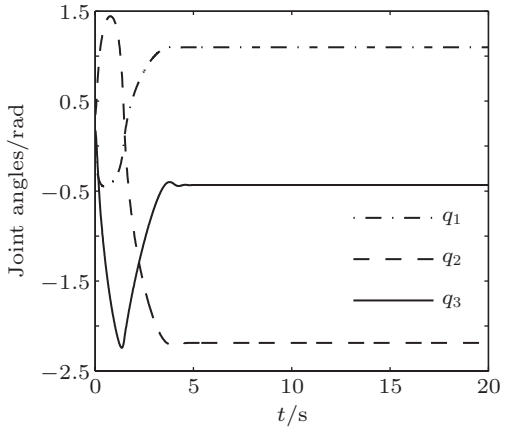


Fig. 6. The joint space trajectories of the RRFTC controller.

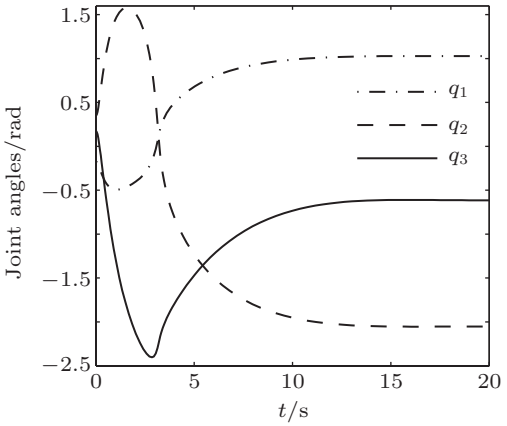


Fig. 7. The joint space trajectories of the RPD controller.

Figures 9–11 show the corresponding control torques of the three controllers. We can see that the required torques of the RFTC ars obviously bigger than the others. The reason may be that a part of the kinetic energy of the manipulator is transferred to the base, which invokes the base motion. Therefore, it is clear that the proposed RRFTC method not only provides a high-precision control performance, but also saves energy.

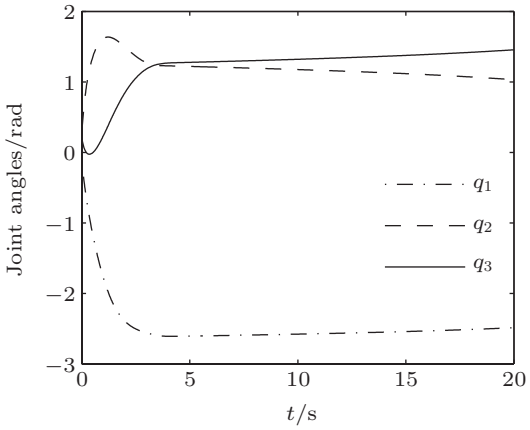


Fig. 8. The joint space trajectories of the RFTC controller.

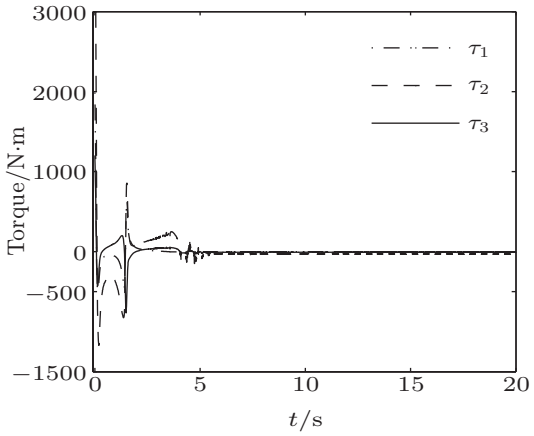


Fig. 9. The required control torques of RRFTC.

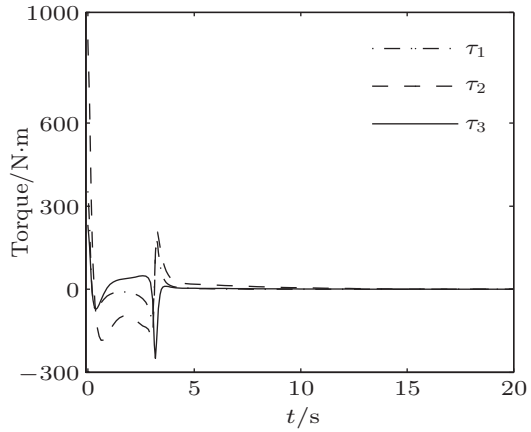


Fig. 10. The required control torques of RPD.

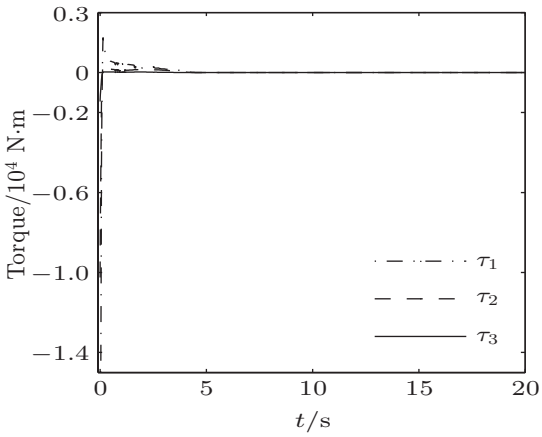


Fig. 11. The required control torques of RFTC.

From the above comparison results, we would like to point out the following.

(i) Full dynamic decoupling of the system in task space is achieved by applying the reaction null space. Via the proposed null space projector, the task space can be decomposed into two complementary orthogonal subspaces. Consequently, control laws for the manipulation of passive objects and the base attitude are designed separately in the two subspaces, such that the complexity of the controller is decreased. Moreover, simultaneous subtask performances are ensured, which means the proposed controller can impose additional force constraints compared with the RFTC, on the base orientation via manipulator motions.

(ii) An outline of high-precision coordinated control is given to the kinematically redundant manipulator. It is vitally important to design a control system with rapid response performance and high precision in view of the on-orbit manipulation. Therefore, a novel frame that combines the reaction null space with the finite-time control is presented to improve the convergence performance. It is clear that the control errors of the proposed controller converge more rapidly and precisely than those of the conventional RPD.

(iii) A nonlinear hyperplane based finite-time control law is developed and applied to the complicated nonlinear system subject to external disturbances. Comparing with the RPD and the RFTC, the proposed closed-loop system shows strong robustness in the presence of bounded uncertain disturbances. Though the simulation is carried out on the two-dimensional case, the proposed controller can be extended easily to the general three-dimensional cases.

5. Conclusion

In this paper, a composite control method capable of manipulating passive objects in task space without inducing disturbances to the base attitude is discussed. The dynamics equation that describes the dynamic coupling behavior of the captured target and the base is derived in the task space. It is shown that decomposition of the dynamics is possible by applying the RNS of the inertia coupling matrix. Therefore, given a redundant manipulator, the reactionless robust finite-time control method is proposed in detail. In addition, a nonlinear robust item is designed to guarantee the global stability in the presence of system uncertainties and external disturbances. Finally, the performance of the proposed control method is examined by comparing with a reactionless PD controller (RPD) and a pure robust finite-time controller (RFTC). The results show that the proposed controller not only keeps the attitude of the base undisturbed, but also manipulates the target to the desired position with higher precision and a shorter settling time. Especially, the proposed method can save energy compared to the controller that does not constrain base rotation. As a result, it is illustrated sufficiently that the proposed controller can satisfy the control requirement of on-orbit manipulation and that it has widespread application prospects in future space missions.

References

[1] Rembala R and Ower C 2009 *Acta Astronaut.* **65** 912
[2] Moosavian S A A and Papadopoulos E 2007 *Robotica* **25** 537
[3] Liao Y, Li D and Tang G 2011 *Sci. China Technol. Sci.* **54** 1234
[4] Sun H, Jia Q, Zhang Q and Wu F 2007 *Electrical Automation* **29** 10 (in Chinese)

[5] Nenchev D N and Yoshida K 1999 *IEEE Tran. Robot. Autmat.* **15** 548
[6] Nenchev D N, Yoshida K, Vichitkulsawat P and Uchiyama M 1999 *IEEE Tran. Robot. Autmat.* **15** 1011
[7] Yoshida K 2003 *Int. J. Robot. Res.* **22** 321
[8] Piersigilli P, Sharf I and Misra A K 2010 *Acta Astronaut.* **66** 183
[9] Oki T, Nakanishi H and Yoshida K 2007 *IEEE/RSJ International Conference on Intelligent Robots and Systems,* October 29–November 2, 2007, San Diego, USA, p. 2256
[10] Dimitrov D N and Yoshida K 2004 *IEEE/RSJ International Conference on Intelligent Robots and Systems,* 2004, Sendai, Japan, p. 3345
[11] Aghili F 2008 *AIAA Guidance, Navigation and Control Conference and Exhibit,* August 18–21, 2008, Honolulu, USA, p. 1
[12] Aghili F 2009 *IEEE/RSJ International Conference on Intelligent Robots and Systems,* October 11–15, 2009, St. Louis, USA, p. 2365
[13] Rekleitis G and Papadopoulos E 2010 *IEEE International Conference on Robotics and Automation,* May 3–8, 2010, Anchorage, USA, p. 2247
[14] Yin S, Ding S X, Haghani A, Hao H and Zhang P 2012 *J. Proc. Control* **22** 1567
[15] Yin S, Luo H and Ding S X 2013 *IEEE Trans. Ind. Electron.* **61** 2402
[16] Rastegari R and Moosavian S A A 2010 *Acta Astronaut.* **66** 748
[17] Khaloozadeh H and Homaeinejad M R 2010 *J. Mech. Sci. Technol.* **24** 1337
[18] Dubowsky S and Papadopoulos E 1993 *IEEE Tran. Robot. Autmat.* **9** 531
[19] Khatib O 1987 *IEEE Tran. Robot. Autmat.* **3** 43
[20] Tortopidis I and Papadopoulos E 2007 *Robotics and Autonomous Systems* **55** 122
[21] Xu W, Liang B, Li C, Xu Y and Qiang W 2007 *Int. J. Adv. Robot. Systems* **4** 17
[22] Khatib O 1995 *Int. J. Robot. Res.* **14** 19
[23] Nenchev D, Umetani Y and Yoshida K 1992 *IEEE Tran. Robot. Autmat.* **8** 1
[24] Hara N, Handa Y and Nenchev D 2012 *IEEE International Conference on Robotics and Automation,* 2012, Saint Paul, USA, p. 299
[25] Huang G, Jiang C and Wang Y 2007 *Acta Phys. Sin.* **11** 6224 (in Chinese)
[26] Yu S, Yu X, Shirinzadeh B and Man Z 2005 *Automatica* **41** 1957
[27] Aghababa M P and Feizi H 2012 *Chin. Phys. B* **21** 060506
[28] Hui L and Li J 2009 *IEEE Trans. Aerosp. Electron. Syst.* **45** 835
[29] Wang X, Si S and Shi G 2006 *Acta Phys. Sin.* **55** 5694 (in Chinese)